IEEE Access
Multidisciplinary : Rapid Review : Open Access Journal

Received January 17, 2021, accepted January 21, 2021, date of publication January 25, 2021, date of current version February 4, 2021.

*Digital Object Identifier 10.1109/ACCESS.2021.3054370*

# Observer-Based Predictive Control of Nonlinear Clutchless Automated Manual Transmission for Pure Electric Vehicles: An LPV Approach

**MOHAMMAD SAEID AKBARI[1], MOHAMMAD HASSAN ASEMANI[1], (Member, IEEE), NAVID VAFAMAND[1], SALEH MOBAYEN[2,3], (Member, IEEE), AND AFEF FEKIH[4], (Senior Member, IEEE)**

[1]School of Electrical and Computer Engineering, Shiraz University, Shiraz 71946-84334, Iran
[2]Future Technology Research Center, National Yunlin University of Science and Technology, Douliu 64002, Taiwan
[3]Department of Electrical Engineering, University of Zanjan, Zanjan 45371-38791, Iran
[4]Department of Electrical and Computer Engineering, University of Louisiana at Lafayette, Lafayette, LA 70504-3890, USA

Corresponding author: Saleh Mobayen (mobayens@yuntech.edu.tw)

**ABSTRACT** This study develops a novel robust control approach for a nonlinear clutchless automated manual transmission (CAMT) in pure electric vehicles. The developed approach comprises model predictive control (MPC), observer, and polytopic linear parameter varying (LPV) model with inexactly measured scheduling parameters. The stability of the online-designed MPC and the offline-designed observer, as well as the overall closed-loop system, is guaranteed by presenting the quadratic Lyapunov function stability conditions in terms of linear matrix inequalities (LMIs). Moreover, by the means of sampler and zero-order-hold (ZOH), the discrete-time LPV-MPC is merged with continuous-time LPV-observer to construct the overall observer-based controller. The first contribution of the presented approach is that the issue of inexactly measured scheduling parameters is considered, which avoids the simplifying separation principal technique. The second contribution is assuring the stability of the closed-loop system with hybrid continuous- and discrete-time systems. Also, the LPV-observer design procedure utilizes the singular value decomposition (SVD) method to reduce the conservativeness; and, a constrained one-step-ahead PV-MPC is suggested. Finally, to illustrate the performance improvement and optimality of the developed controller, it is applied to a nonlinear CAMT system and comparison numerical results are given.

**INDEX TERMS** Polytopic LPV system, inexact scheduling parameters, observer-based control, model predictive control (MPC), linear matrix inequality, clutchless automated manual transmission, pure electric vehicle.

## I. INTRODUCTION

Among the electric vehicles, the Pure Electric Vehicle (PEV) benefits from the consumption of completely clean electric power. Deploying the highly precise and effective electric motors in PEVs brings new challenges and occasions in transferring power to the wheels [1]–[3]. The power transmission structure of PEVs can be principally classified as Distributed Motor-Driven (DMD) and Centralized Motor-Driven (CMD) [4]. In the first category, the powertrain structure does not need mechanical transmission and differential, and PEVs are directly actuated by in-wheel motors. However, several apparatuses should be installed at the wheels, which increases the wheel un-sprung mass and vibration acceleration, and degrades the riding quality and comfort [5]. Besides, the second category has almost the same apparatus as the conventional power transmission systems with the exception that the inter-combustion engine is removed and the electric motors are installed [6]. Compared with the DMD PEV technology, the CMD PEV has been widely utilized in the industry because of its inheritance similarity with the conventional propulsion systems [6]. Also, in the CMD PEVs, by eliminating the clutch control mechanism, an enhanced and more smoothed shifting is achieved by actively controlling the electric motors. Thus, it is preferred to deploy gears with a fixed gear ratio to control most industrial

The associate editor coordinating the review of this manuscript and approving it for publication was Ahmed F. Zobaa.

PEVs' speed and simplify the powertrain structure [4]. In contrast with the dual-clutch, conventional automated, continuously variable transmission methods, the high efficiency and the low weight and cost of the Clutchless Automated Manual Transmission (CAMT) make it a proper choice in the centralized motor-driven PEV automated transmission [7], [8]. The CAMT has already been exposed to effectively enhance the drivability and energy efficiency of pure electric buses.

The CAMT in the centralized motor-driven PEVs has fast dynamics in which driveline oscillations appear. This fact makes the overall speed control of PEVs more challenging [9], [10]. In recent years, various control approaches have been proposed for the speed control of PEVs using CAMT. In [11], the nonlinearity of the air drag force has been represented by a Takagi-Sugeno fuzzy model and the scheduling parameters are estimated using an observer. However, it is assumed that the aerodynamic gains are known. In [12], the dynamics of the CAMT are analyzed and a gear-shifting controller is presented for the enhanced position regulation performance of gear-shifting actuators. In [13], a robust $H_\infty$ Linear Quadratic Regulator (LQR) is incorporated with the pole-placement technique to alleviate the effect of the external load torque on the speed of PEV. A robust performance improvement with two-layer control scheme in four-wheel electric vehicle is proposed in [14]. In [15], a recursive least-squares algorithm is considered to update the parameters of a brushless DC motor, then a generalized Proportional Integral (PI) approach is developed for the speed synchronization of CAMT systems in the presence of networked induced delays. In addition, an unknown input observer control scheme is considered in [16] for the estimation of the states of CAMT. Then, the gain of the Kalman-Bucy filter is deployed to eliminate the effect of the torque disturbance on the estimation. In [17], the problem of the CAMT is investigated to improve the system performance of down- and up-shifts. In [18], a two-motor PEV CAMT dynamics is considered and the problem of torque control for multiple speed gear ratio issue is investigated. Besides, an event-triggered robust $H_\infty$ state-feedback controller with two performance indices is designed in [4] via Linear Matrix Inequalities (LMIs). The so-called performance indices stand for wheel speed (to assure the tracking performance) and the axle wrap rate (to assure the passenger comfort), respectively. The attempt is made to reduce the effect of the external disturbance based on the energy-to-peak criterion. In [11], the nonlinearity of the air drag force is modeled by a Takagi-Sugeno fuzzy representation and then an observer is presented to estimate the scheduling parameters. Utilizing Vehicle-to-Grid technique, EVs can act as loads. [19] investigates aggregation of EVs for frequency control of microgrid by implementing grid regulation and charger controller.

During the last decades, Linear Parameter Varying (LPV) Model Predictive Control (MPC) methods have received a great deal of consideration due to their practical implementation [9], [10], [20]. For applications with all state variables not available from measurement, the output-feedback robust MPC is the solution of choice. However, it is worth noting that no common valid separation principle exists to affirm the stability of the augmented closed-loop system in output-feedback robust MPC. This is due to the existence of physical constraints along with the coupling between the parameters of the observer and controller [21]. Most of the recent advances in output-feedback robust MPC for LPV stabilize the augmented closed-loop system by simultaneously optimizing the parameters of the observer and controller. Hence, in order to attain robust stability while satisfying the given constraints, one must take into consideration the joint dynamics of the observer and the controlled system. A major drawback of this technique, however, is the Bilinear Matrix Inequality (BMI) problem; a nonconvex optimization approach that cannot be solved in polynomial time [22], [23]. In [24], [25], quadratic boundedness is considered to guarantee that the current and future augmented states are constrained in one Robust Positive Invariant (RPI) set such that the robust stability of the augmented closed-loop system is ensured. An N-step MPC for Systems with Persistent Bounded disturbance under SCP is discussed in [26]. The off-line output-feedback robust MPC technique based on a look-up table approach is studied in the researches of Ping and Ding [24] for decreasing the online computational burden. The state-observer gain is first designed off-line. The gain of the online optimized controller is then determined by considering the dynamics of the estimation error, computed using the off-line observer gain, so as to avoid the coupling between the observer and controller gains. Note, however, that those gains are derived with the assumption that the scheduling parameters are completely known. The problem of designing resilient MPC for cyber-physical systems (CPSs) has been addressed in [27]. The design took into consideration the polytopic uncertainties and state saturation nonlinearities under the Try-Once-Discard (TOD) scheduling. For the inexact scheduling parameters of LPV systems, the nonconvex optimization problems have been solved using an iterative Cone Complementarity Linearization (CCL) algorithm in [28]. However, the considered approach resulted in conservative solutions due to the use of CCL.

In general, in the experimental cases, there is mismatch between the actual and measured values depending on sensor error and imprecision because of calibration, temperature variation, and quality of instrument. This issue has become a stimulating research topic and numerous techniques have been planned for LPV systems with inexactly measured scheduling parameters in several themes, covering design of fault-detection observer [29], filtering [30], design of state-feedback controller [31], and design of output-feedback controller [32]. Since in the practical circumstances, the states are not available for feedback control, this work emphases on design of the output-feedback control technique. In [33] and [34], the topics of designing a dynamic output-feedback controller and an observer-based controller are considered, respectively. However, in those approaches, the existence of uncertainties in the scheduling parameters is not studied. In a few references, the inexact scheduling parameter issue has been investigated in [35] and [36]. For example in [35], the design conditions of an observer-based controller are presented in terms of LMIs by considering that the scheduling parameter measurements get different values from their real ones due to parametric uncertainties. The results of [35] are then improved in [36], where the observer-based controller is extended to a more general class. However, in [35] and [36], the inexact parameters are supposed to be proportional to their real values. Recently in [37], the observer-based controller, which does not expose any restriction on the inexact parameters is suggested. Though, in that approach, the controller is designed offline without considering any constraint on the system states and control inputs.

In this paper, a novel observer-based MPC design method is proposed to deal with the inexactly measured scheduling parameters for the nonlinear CAMT systems represented by polytopic LPV systems. To formulate the design conditions by LMIs, a novel method based on the Singular Value Decomposition (SVD) form of the output matrix is proposed. Such an approach avoids the well-known problem of appearing equality constraints in the observer-based controller design procedure [38] and makes the constraints procedure convex. The LMI conditions not only guarantee the stability of the closed-loop system, but also ensure the desired level of its induced $L_2$-norm in the existence of any external disturbances and inexact scheduling parameters. Also, a constrained one-step-ahead MPC is developed. Since the gain-scheduling parameters are not completely known, the observer and controller design procedure does not fulfill the separation principle. Also, in order to have an accurate controller, a continuous-time observer is designed offline, meanwhile, the discrete-time MPC is developed online. Though, the interactions between the observer and controller are considered in the design procedure to assure closed-loop stability. Finally, several simulations and comparisons are provided to demonstrate the applicability and effectiveness of the proposed approach for a CAMT case study.

This paper is structured as follows. Section II provides the dynamics of practical CAMT of PEV and derives its polytopic LPV representation. Section III details the proposed LPV-based MPC and LPV-based observer. Section IV illustrates the simulation results and comparison study with state-of-the-art methods. Finally, some concluding remarks are given in section V.

## II. PRACTICAL CAMT OF PEV

### A. DRIVELINE DYNAMICS

The CAMT is mainly comprised of the motor-gearbox and wheel-vehicle apparatus, which are commonly modeled as signal inertia systems shown in Figure. 1 [39]. Whenever the transmission gears are engaged, then the following relations hold:

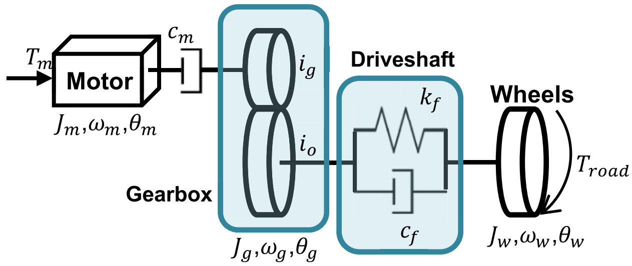


**FIGURE 1. Simplified schematic of the driveline.**

$$T_{go} = i_g i_o T_{gi}, \quad \omega_m = i_g i_o \omega_g, \quad \theta_m = i_g i_o \theta_g, \tag{1}$$

where $i_g$ and $i_o$ are the gear and final drive ratios, respectively, $T_{gi}$ is the torque input to the gearbox, $T_{go}$ is the torque output of the gearbox, $\theta_m(\omega_m)$ and $\theta_q(\omega_g)$ are the motor and gearbox output angles (rotations), respectively.

Considering (1), the dynamics of the CAMT system are represented as follows [4], [11]:

$$\begin{cases} J_{mg}\dot{\omega}_m = T_m - T_f/i_g i_o - c_m\omega_m \\ J_v\dot{\omega}_w = T_f - T_{road} \\ J_{mg} = J_m + J_g/i_g^2 i_o^2 \\ T_f = c_f\left(\omega_m/i_g i_o - \omega_w\right) + k_f\left(\dfrac{\theta_m}{i_g i_o} - \theta_w\right) \end{cases} \tag{2}$$

where $J_m$ is the inertia of the driving motor, $J_g$ is the gearbox inertia, $J_v$ is the vehicle inertia, which can be obtained by adding the wheels' inertia $J_w$ to the equivalent inertia of the vehicle mass $m_v$. $T_m$ is the motor torque, $T_f$ is the torque in the flexible driveshaft, $\omega_w$ is the rotation speed of the wheel, $c_m$ is the damping coefficient of the motor, $c_f$ is the drive shaft damping coefficient, $k_f$ is the stiffness factor, and $C_r$ is the rolling resistance coefficient. $T_{road}$ is the external load torque including airdrag $T_{airdrag}$, rolling torque $T_{roll}$ and resistant torque $T_{grad}$ due to the road grade, which is defined by

$$\begin{aligned} T_{road} &= T_{roll} + T_{grad} + T_{airdrag}, T_{roll} = C_r m_v g cos\left(\alpha\right) r_w, \\ T_{grad} &= m_v g sin\left(\alpha\right) r_w, T_{airdrag} = \frac{1}{2}\rho_{air} A_f C_d r_w^3 \omega_w^2. \end{aligned} \tag{3}$$

where $\alpha$ is the road grad, $r_w$ is the wheel radius, $\rho_{air}$ is the air density, $A_f$ is the frontal area of the vehicle, $C_d$ is the airdrag coefficient.

### B. POLYTOPIC-LPV REPRESENTATION

To derive the polytopic-LPV representation, the external load torque is decomposed as

$$\begin{aligned} T_{road} &= T_{airdrag} + T_{roll} + T_{grad} \\ &= \frac{1}{2}\rho_{air} A_f C_d r_w^3 \omega_w^2 + w\left(t\right). \end{aligned} \tag{4}$$

where $T_{roll} + T_{grad}$ is taken as $w(t)$ which is an external disturbance vector whose elements belong to $L_2$ and

$L_\infty$ spaces. Furthermore, for the desired wheel angular speed reference $\omega_w^*$, the tracking error vector and the new control input are obtained as $\tilde{x}(t) = \left[\tilde{x}_1(t)\tilde{x}_2(t)\tilde{x}_3(t)\right]^T$ and $u(t) = T_m - T_M^*$, where $\tilde{x}_1(t) = \omega_m - \omega_m^*$, $\tilde{x}_2(t) = \omega_w - \omega_w^*$, and $\tilde{x}_3(t) = (\theta_m/i_g i_o - \theta_w) - (\theta_m^*/i_g i_o - \theta_w^*)$, where

$$\begin{cases} \omega_m^* = i_g i_o \omega_w^* \\ \dfrac{\theta_m^*}{i_g i_o} - \theta_w^* = \dfrac{1}{2k_f}\rho_{air} A_f C_d r_w^3 \omega_w^* 2 \\ T_m^* = c_m i_g i_o \omega_w^* + \dfrac{1}{2 i_g i_o}\rho_{air} A_f C_d r_w^3 \omega_w^* 2 + \dfrac{w^*}{i_g i_o}. \end{cases} \tag{5}$$

The tracking error dynamics are obtained based on (2)-(5), as follows:

$$\dot{\tilde{x}}(t) = A(t)\,\tilde{x}(t) + Bu(t) + Ew(t), \tag{6}$$

with

$$A(\theta(t)) = \begin{bmatrix} \frac{c_f - i_g^2 i_o^2 c_m}{J_{mg} i_g^2 i_o^2} & \frac{c_f}{J_{mg} i_g i_0} & -\frac{k_f}{J_{mg} i_g i_0} \\ \frac{c_f}{J_v i_g i_o} & \left\{ \begin{array}{c} -\frac{c_f}{J_v} - \frac{1}{2J_v}\rho_{air} A_f \\ \times C_d r_w^3 (2\omega_w^* + \tilde{x}_2(t)) \end{array} \right\} & \frac{k_f}{J_v} \\ \frac{1}{i_g i_o} & -1 & 0 \end{bmatrix},$$

$$B_2 = \begin{bmatrix} \frac{1}{J_{mg}} \\ 0 \\ 0 \end{bmatrix}, E = \begin{bmatrix} 0 \\ -\frac{1}{J_v} \\ 0 \end{bmatrix}, \tag{7}$$

where $u(t)$ denotes the control input and $w(t)$ indicates the disturbance. The term $\frac{1}{2J_v}\rho_{air} A_f C_d r_w^3 (2\omega_w^* + \tilde{x}_2(t))$ comprises the uncertain time-varying parameters $\rho_{air}$, $C_d$, $A_f$, the state $\tilde{x}_2(t)$, and desired cruise speed $\omega_w^*$. Thereby, the dynamics (6) should be rewritten by a polytopic-LPV model. Because the PEV speed is limited and the varying parameters are bounded, one has

$$\underline{\theta} \le \frac{1}{2}\rho_{air} A_f C_d r_w^3 \left(2\omega_w^* + \tilde{x}_2(t)\right) < \bar{\theta}, \tag{8}$$

where $\underline{\theta}$ and $\bar{\theta}$ are the lower and upper bounds, respectively.

Applying the sector nonlinearity approach, a two-vertex polytopic-LPV system is obtained as

$$\begin{cases} \dot{\tilde{x}}(t) = \displaystyle\sum_{i=1}^{2} \rho_i(\theta(t)) \{A_i \tilde{x}(t) + Bu(t) + Ew(t)\} \\ y(t) = \tilde{x}_2 = C\tilde{x}(t) \end{cases} \tag{9}$$

where $\theta(t) = \frac{1}{2}\rho_{air} A_f C_d r_w^3 (2\omega_w^* + \tilde{x}_2)$. Also,

$$A_1 = \begin{bmatrix} \dfrac{c_f - i_g^2 i_o^2 c_m}{J_{mg} i_g^2 i_o^2} & \dfrac{c_f}{J_{mg} i_g i_0} & -\dfrac{k_f}{J_{mg} i_g i_0} \\ \dfrac{c_f}{J_v i_g i_o} & -\dfrac{c_f + \underline{\theta}}{J_v} & \dfrac{k_f}{J_v} \\ \dfrac{1}{i_g i_o} & -1 & 0 \end{bmatrix},$$

$$A_2 = \begin{bmatrix} \dfrac{c_f - i_g^2 i_o^2 c_m}{J_{mg} i_g^2 i_o^2} & \dfrac{c_f}{J_{mg} i_g i_0} & -\dfrac{k_f}{J_{mg} i_g i_0} \\ \dfrac{c_f}{J_v i_g i_o} & -\dfrac{c_f + \bar{\theta}}{J_v} & \dfrac{k_f}{J_v} \\ \dfrac{1}{i_g i_o} & -1 & 0 \end{bmatrix},$$

$$\rho_1(\theta(t)) = \frac{\bar{\theta} - \theta(t)}{\bar{\theta} - \underline{\theta}}, \rho_2(\theta(t)) = 1 - \rho_1(\theta(t)),$$
$$C = \begin{bmatrix} 0 & 1 & 0 \end{bmatrix}. \tag{10}$$

Moreover, the available output $y(t)$ in (9) is obtained by measuring the wheel speed $\omega_m$ and involving the desired reference $\omega_m^*$. It should be remarked that the exact value of $\theta(t)$ is not available, since it is a function of time-varying aerodynamics parameters $\rho_{air}$, $A_f$, $C_d$, and $r_w$. This practical issue makes the time-varying parameters inexactly measurable.

Our objective is to design a robust controller against the external disturbance to assure the regulation of the speed of PEV to its desired value in the presence of practical constraints and the above-mentioned challenges. To achieve this goal, an observer-based LPV-MPC is suggested in this paper. In the following section, our proposed approach will be discussed.

## III. ROBUST LPV OBSERVER-BASED PREDICTIVE CONTROLLER DESIGN

This section deals with designing a nonlinear MPC controller to assure the stability of the closed-loop system. The MPC approach is inherently developed for discrete-time systems. On the other hand, an observer should be designed to deal with the inexactly measurable time-varying parameters and state estimations of the continuous-time system. This contradiction encourages the design of the overall controller design into the following two steps:

### A. ROBUST LPV-BASED PREDICTIVE CONTROLLER DESIGN

Consider a class of discrete-time LPV model of the following form:

$$\begin{aligned} x(k+1) &= \bar{A}(\theta(k))\,x(k) + \bar{B}u(k) + \bar{E}\bar{w}(k) \\ y(k) &= Cx(k) \end{aligned} \tag{11}$$

where $\bar{A}(\theta(k))$, $\bar{B}$, and $\bar{E}$ can be obtained by discretizing the system (6). Furthermore, $x(k)$, $u(k)$, $\bar{w}(k)$, $y(k)$ are the discrete states, control input, disturbance, and output vector. Assume that the state vector is measurable. Also, the matrix $\bar{E}$ should be chosen so that the following assumption holds:

*Assumption 1:* The disturbance term $\bar{w}(k)$ is persistent, bounded, and satisfies

$$\|\bar{w}(k)\| \le 1 \tag{12}$$

Moreover, there exist non-negative coefficients $\rho_l(\theta(k))$, $l \in \{1, \ldots, p\}$, such that $\sum_{l=1}^{p} \rho_l(\theta(k)) = 1$ and $A(\theta(k)) = \sum_{l=1}^{p} \rho_l(\theta(k)) A_l$. The input is subject to the following constraint

$$-\bar{u} \leq u(k) \leq \bar{u} \tag{13}$$

The computational time for solving the MPC control problem is assumed to be less than one sampling interval. The following one-step ahead feedback control law is utilized [40]:

$$u(k+i\,|\,k) = \begin{cases} F(k-1)\,x(k+i\,|\,k), & i=0 \\ F(k)\,x(k+i\,|\,k), & \forall i>0 \end{cases} \tag{14}$$

In order to bound the state in the presence of unknown disturbance, the concept of robust positive invariance is utilized.

*Definition 1.* A convex set $\Omega$ is a Robust Positive Invariant (RPI) for the time-varying system $x(k+1) = f(x(k), w(k))$, if for all $w(k) \in W$, $x(k) \in \Omega$ implies $x(k+1) \in \Omega$ for all $k > 0$.

*Theorem 1.* For the system (16) with feedback control law (14), the terminal region $X_f(k) = \{x|\, V(x,k) \leq 1\}$, where $V(x,k) = x(k)^T Q^{-1} x(k)$, is an RPI set in the presence of disturbance $\bar{w}(k)$ satisfying Assumption 1, if there exist scalars $\alpha \in (0, 1]$ and $\beta$ such that

$$\min_{\gamma,Q,Y,Z}, \gamma \tag{15}$$

subject to

$$\begin{bmatrix} (1-\alpha)Q & \star & \star & \star & \star \\ 0 & \alpha & \star & \star & \star \\ A_l Q + BY & E & Q & \star & \star \\ L^{1/2}Q & 0 & 0 & \gamma I & \star \\ R^{1/2}Y & 0 & 0 & 0 & \gamma I \end{bmatrix} \geq 0, \quad \forall l \in \{1, 2, \ldots, p\} \tag{16}$$

$$\begin{bmatrix} 1-\beta & \star & \star \\ 0 & \beta I & \star \\ (A_l + B_l F(k-1))\,x(k) & E_l & Q \end{bmatrix} \geq 0, \tag{17}$$

$$\begin{bmatrix} Q & \star \\ Y & Z \end{bmatrix} \geq 0, Z^{(j)} \leq \bar{u}_j^2 \quad \text{for } j = 1, \ldots, n_u \tag{18}$$

where $\gamma$ is a suitable nonnegative variable to be minimized, $Z^{(j)}$ stands for the $j$-th array of the diagonal element, and $\bar{u}_j$ represents the peak bound of the $j$-th control input. Finally, $F(k) = YQ^{-1}$.

*Proof:* In order to guarantee the stability of the system (11) with control law (14) in the presence of disturbance, we utilize the concept of Quadratic Boundedness (QB) [24] to fulfill that $X_f(k) = \{x|\, V(x,k) \leq 1\}$ is a RPI set if the following condition is satisfied:

$$\text{if } V(x,i\,|\,k) \geq 1 \Longrightarrow V(x,i+1\,|\,k) \leq V(x,i\,|\,k),\ \forall i>0 \tag{19}$$

The conventional RPI method can be extended to the optimal controller design as

$$\begin{aligned} &V(x,i+1\,|\,k) - V(x,i\,|\,k) \leq -1/\gamma \\ &\left[x(k+i\,|\,k)^T Lx(k+i\,|\,k) + u(k+i\,|\,k)^T Ru(k+i\,|\,k)\right], \\ &\forall i>0 \end{aligned} \tag{20}$$

where $L$ and $R$ are the weights of the cost function

$$\begin{aligned} J(k) = \sum_{\forall i>0} & x(k+i\,|\,k)^T Lx(k+i\,|\,k) \\ & + u(k+i\,|\,k)^T Ru(k+i\,|\,k). \end{aligned} \tag{21}$$

and $\gamma$ is the upper bound of the cost function. Since $\|\bar{w}(k)\| \leq 1$ and $V(x,i+1\,|\,k) \geq 1$, one concludes $V(x,i+1\,|\,k) \geq \bar{w}(k)^T \bar{w}(k)$. Then, by applying the S-procedure, we have

$$\begin{aligned} &V(x,i+1\,|\,k) - V(x,i\,|\,k) \\ &\quad -\alpha\left(\bar{w}(k)^T \bar{w}(k) - V(x,i+1\,|\,k)\right) \\ &\quad +1/\gamma\left[x(k+i\,|\,k)^T Lx(k+i\,|\,k)\right. \\ &\quad \left.+u(k+i\,|\,k)^T Ru(k+i\,|\,k) \leq 0,\right] \\ &\quad \forall i>0 \end{aligned} \tag{22}$$

where $\alpha > 0$ is an arbitrary scalar value. By arranging (22) in a quadratic form in terms of $[x(k+i\,|\,k)\,\bar{w}(k)]^T$, defining $Y = F(k)\,Q$, and applying Schur complement, (16) is obtained.

On the other hand, one needs to guarantee $x(k+1\,|k) \in X_f(k)$ for all possible $\bar{w}(k)$ satisfying $\|\bar{w}(k)\| \leq 1$, as

$$\left\{\|\bar{w}(k)\| \leq 1 \rightarrow x(k+1\,|k) \in X_f(k)\right\}. \tag{23}$$

By utilizing (11) and (14) and applying S-procedure on (23), we obtain

$$\begin{aligned} &1 - \beta - \left[(A_l + B_l F(k-1))\,x(k) + \bar{E}\bar{w}(k)\right]^T Q^{-1} \left[(A_l\right. \\ &\quad \left.+ B_l F(k-1))\,x(k) + \bar{E}\bar{w}(k)\right] + \beta w(k)^T E_l^T E_l w(k) \geq 0. \end{aligned} \tag{24}$$

By expressing (24) in a quadratic form in terms of $[1 w(k)^T]$ and eliminating the variables, it is shown that (24) is equivalent to

$$\begin{aligned} &\begin{bmatrix} 1-\beta & \star \\ 0 & \beta \end{bmatrix} - \begin{bmatrix} [(A_l + B_l F(k-1))\,x(k)]^T \\ E_l^T \end{bmatrix} \\ &\quad \times Q^{-1}\left[\,(A_l + B_l F(k-1))\,x(k) \quad E_l\right] \geq 0 \end{aligned} \tag{25}$$

By applying the Schur complement on (25), (17) is obtained. On the other hand, in order to handle the constraint on the control input $u(k)$, the constraint on the future control sequence $u(k+1\,|\,k)$ needs to be considered. For this constraint, consider the peak bounds [41]

$$\left|u_j(k+i\,|\,k)\right| < \bar{u}_j, \quad j = 1, 2, \ldots, n_u, \quad i \geq 1 \tag{26}$$

where it holds that

$$\begin{aligned} \max_{i\geq1} \left|u_j(k+i\,|\,k)\right|^2 &= \max_{i\geq1} \left|\left(YQ^{-1}x(k+i\,|\,k)\right)_j\right|^2 \\ &\leq \left\|\left(YQ^{-1/2}\right)_j\right\|_2^2 = \left(YQ^{-1}Y^T\right)_{jj} \end{aligned} \tag{27}$$

If there exists a symmetric matrix $Z$ such that (18) holds, (26) is assured. The proof is complete. ■

### B. LPV-BASED OBSERVER DESIGN

In a practical CAMT, the measurement of all states is costly and increases the volume of the PEV gearbox. So, it is preferred to estimate the state-vector based on the available measures [42], [43]. In this regard, the term $x(k+i|k)$ of the control law (14) should be replaced by the term $\hat{x}(k+i|k)$. To compute $\hat{x}(k+i|k)$, define the following polytopic observer:

$$\begin{cases} \dot{\hat{x}}(t) = A\left(\hat{\theta}(t)\right)\hat{x}(t) + Bu(t) + L\left(\hat{\theta}(t)\right)\left(y(t) - \hat{y}(t)\right) \\ \hat{y}(t) = C\hat{x}(t) \end{cases} \tag{28}$$

where $\hat{\theta}(t)$ is the vector of inexact measured scheduling parameters, where $\hat{\theta}(t) \neq \theta(t)$. However, the polytopic vertices for the system and the observer are equal. This paper does not exert any conservative relationship between the time-varying scheduling parameters and their inexact measurements. Whereas the scheduling parameters satisfy $\underline{\theta}_i \leq \theta_i(t) \leq \bar{\theta}_i$, the inexactly measured scheduling parameters should only satisfy similar bounds, as

$$\underline{\theta}_i \leq \hat{\theta}_i(t) \leq \bar{\theta}_i, \quad i = 1, 2, \ldots, p. \tag{29}$$

Referring to Figure.2, the inexactly measured scheduling parameters get any values in the colored hyper-rectangular Region 1 characterized by vertices $\underline{\theta}_i$ and $\bar{\theta}_i$. However, if they get any value in Regions 2 and 3, they will be replaced by $\bar{\theta}_i$ and $\underline{\theta}_i$, respectively. It is noted that all observer design methods considering inexact scheduling parameters exploit the online measured values of parameters, which can be perturbed and different from their real values.

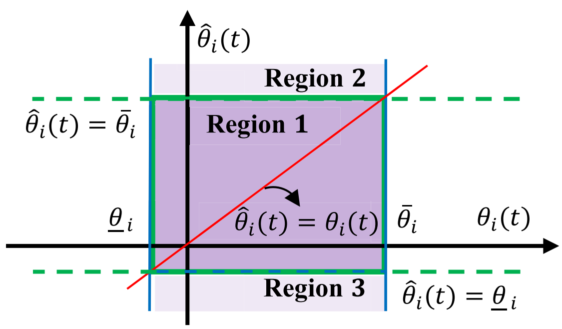


**FIGURE 2.** Admissible region for the measured scheduling parameters.

The dynamics of $e(t) = \tilde{x}(t) - \hat{x}(t)$ are obtained as

$$\dot{e}(t) = \left(A(\theta(t)) - L\left(\hat{\theta}(t)\right)C\right)e(t) + \left(A(\theta(t)) - A\left(\hat{\theta}(t)\right)\right)\hat{x}(t) + Ew(t). \tag{30}$$

Further, one has

$$\dot{\hat{x}}(t) = \left(L\left(\hat{\theta}(t)\right)C\right)e(t) + \left(A\left(\hat{\theta}(t)\right) - BF\right)\hat{x}(t). \tag{31}$$

where $F$ is the controller gain. Augmetnig (30) and (31) as $x_{cl}(t) = \left[\hat{x}(t)^T e(t)^T\right]^T$, it follws that

$$\dot{x}_{cl}(t) = A_{cl}\left(\theta(t), \hat{\theta}(t)\right)x_{cl}(t) + E_{cl}w(t) \tag{32}$$

$$z(t) = C_{cl}x_{cl}(t), \tag{33}$$

with

$$A_{cl}\left(\theta(t), \hat{\theta}(t)\right) = \begin{bmatrix} A\left(\hat{\theta}(t)\right) - BF & L\left(\hat{\theta}(t)\right)C \\ A(\theta(t)) - A\left(\hat{\theta}(t)\right) & A(\theta(t)) - L\left(\hat{\theta}(t)\right)C \end{bmatrix}, \tag{34}$$

$$E_{cl} = \begin{bmatrix} 0 \\ E \end{bmatrix}, \tag{35}$$

$$C_{cl} = \begin{bmatrix} C & C \end{bmatrix}, \tag{36}$$

*Lemma 1 [44]:* For the following LPV system:

$$\begin{aligned} \dot{x}(t) &= A(\theta(t))x(t) + B(\theta(t))w(t) \\ y(t) &= C(\theta(t))x(t) + D(\theta(t))w(t) \end{aligned}, \tag{37}$$

and any matrix $X = X^T > 0$, the $H_\infty$ performance criterion $\gamma$ can be specified by

$$\begin{bmatrix} A(\theta(t))X + XA^T(\theta(t)) & * & * \\ B^T(\theta(t)) & -\gamma^2 I & * \\ C(\theta(t))X & D(\theta(t)) & -I \end{bmatrix} < 0, i = 1, \ldots, p. \tag{38}$$

*Theorem 2:* The system (32) characterized by $C = U[S \quad 0]V^T$ is stable with $\gamma$ attenuation level, if there exist symmetric positive matrices $X_1$, $X_{11}$, and $X_{22}$ and matrices $Z_j$ and $M$ fullfilling

$$\begin{bmatrix} \begin{pmatrix} A_jX_1 - BM+ \\ X_1A_j^T - MB^T \end{pmatrix} & * & * & * \\ \begin{pmatrix} (A_i - A_j)X_1 \\ -C^TZ_j^T \end{pmatrix} & \begin{pmatrix} A_iX_2 - Z_jC \\ +X_2A_i^T - C^TZ_j^T \end{pmatrix} & * & * \\ 0 & B^T & -\gamma^2 I & * \\ CX_1 & CX_2 & 0 & -I \end{bmatrix} < 0, i, j = 1, \ldots, p \tag{39}$$

where $X_2 = V\begin{bmatrix} X_{11} & 0 \\ 0 & X_{22} \end{bmatrix}V^T$. The observer gains are given by

$$L_j = Z_j\bar{X}_2^{-1} \tag{40}$$

*Proof.* Using Lemma 1 and (32), if there exists a matrix $X = X^T > 0$ such that

$$\begin{bmatrix} \begin{Bmatrix} A_{cl}(\theta(t), \hat{\theta}(t))X+ \\ XA_{cl}^T(\theta(t), \hat{\theta}(t)) \end{Bmatrix} & * & * \\ B_{cl}^T(\theta(t)) & -\gamma^2 I & * \\ C_{cl}(\theta(t), \hat{\theta}(t))X & 0 & -I \end{bmatrix} < 0. \tag{41}$$

Then, by partitioning $X$ as $X = \mathrm{diag}(X_1, X_2)$, (41) results in (42), as shown at the bottom of the next page.

Let the output matrix to be represented in the singular value decomposition (SVD) form $C = U[S \quad 0]V^T$, where $S$ is a diagonal matrix, 0 is a zero matrix and, $U$ and $V$ are unitary matrices. Inspired from [45], for $X_2 = V\begin{bmatrix} X_{11} & 0 \\ 0 & X_{22} \end{bmatrix}V^T$, there exists $\bar{X}_2 = USX_{11}S^{-1}U^{-1}$ that satisfies $CX_2 = \bar{X}_2C$. By defining the changes in the variables $M = FX_1$ and $Z_j = L_j\bar{X}_2$, (42) leads to (39). This thereby completes the proof. ■

### *C. INTEGRATION OF MPC AND OBSERVER*

As can be seen in Sections 3.1 and 3.2, the LPV-MPC should be designed discrete-time. However, the closed-loop system should be implemented in a continuous-time form. The overall proposed observer-based MPC schematic is illustrated in Figure. 3. The discrete-time MPC is implemented by adding a sampler and zero-order-hold (ZOH). Further, since both the observer and the MPC are designed for dynamic error, it is necessary to compute the tracking error output $y(t)$ and the actual control input $T_m$ based on the desired references for the wheel speed (i.e., $\omega_M^*$) and control input bias (i.e., $T_M^*$).

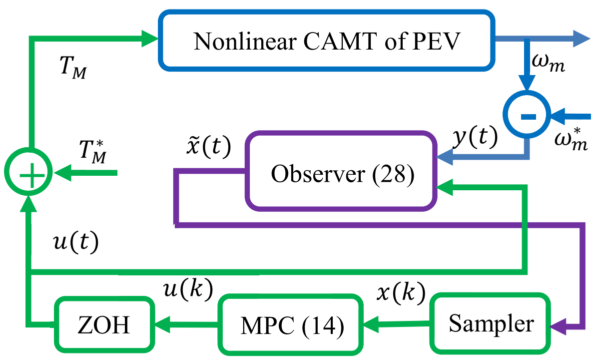


**FIGURE 3.** **The closed-loop system schematic.**

Since the overall system, LPV-observer, and the LPV-MPC are nonlinear, the separation principle is not held and the effects of observer and MPC on each other should be considered to achieve the overall stability. The observer (28) is designed offline. On the other hand, the gains of MPC (i.e. $F(k)$) are designed online. Thereby, the controller gain is not available at the stage of designing the observer (28). In order to solve this issue, additional constraints should be added to Theorems 1 and 2 to make the overall closed-loop system stable. From (42), one infers that

$$\text{Const1} : \left(A_j - BF\right) X_1 + X_1 \left(A_j^T - F^T B^T\right) < 0 \quad (43)$$

which verifies that the continuous-time non-disturbed closed-loop system $(A, B)$ (with the control $u = Fx$) must be stable. However, the gains $F$ in the online MPC optimization will be computed optimal later. If the control gains of MPC, besides the conditions of Theorem 1, are found such that the eigenvalues of $(A, B)$ are smaller than those of Const1 in (16), then the observer will be stable for the gains of MPC. In other words, for any $F^*$ which satisfies (42), if there exists $F(k)$ that guarantees

$$\left(A_j - BF(k)\right) < \left(A_j - BF^*\right) \quad (44)$$

then, (42) will be held. The extra constraint (44) can affect the optimal solution of LPV-MPC and Theorem 1. In order to reduce this effect, it is required to find $F^*$ so that Const1 is non-strictly feasible. In this regard, the following optimization problem should be added to Theorem 2:

$$F^* = \min \sigma$$

Subject to:

$$-\sigma I \leq \left(A_j - BF\right) X_1 + X_1 \left(A_j^T - F^T B^T\right). \quad (45)$$

Then, for the feasible solution of $F^*$, the following constraint should be added to Theorem 1:

$$A_j - BF\,(k) \leq \lambda_{min}\left(A_j - BF^*\right) I = \varepsilon I, \quad (46)$$

or equivalently

$$A_j - BF\,(k) - \varepsilon I \leq 0 \quad (47)$$

Considering $V = x^T Q^{-1} x$ with $Q > 0$, its time-derivative results:

$$Q^{-1}\left(A_j - BF\,(k) - \varepsilon I\right) + \left(A_j^T - F\,(k)^T B^T - \varepsilon I\right) Q^{-1} \leq 0 \quad (48)$$

Reminding $F\,(k) = YQ^{-1}$, (48) is continued as satisfied by

$$Q^{-1}A_j + A_j^T Q^{-1} - 2\varepsilon Q^{-1} - Q^{-1}BYQ^{-1} - Q^{-1}Y^T B^T Q^{-1} \leq 0. \quad (49)$$

Pre- and post-multiplying (49) by $Q$, one gets

$$A_j Q + Q A_j^T - 2\varepsilon Q - BY - Y^T B^T \leq 0. \quad (50)$$

By adding LMI (50) to Theorem 1, the controller gains $F(k)$ are obtained such that the stability of the observer is guaranteed.

The flowchart of the proposed controller design procedure is presented in Figure 4. As can be seen in Figure 4, the observer gains are obtained offline based on the continuous-time system representation and LMIs (39) of Theorem 2 and the optimization (45). Furthermore, the MPC controller gains are computed for the discrete-time representation of the system via the optimization problem (15)-(18) of Theorem 1 (to assure the stability of the constrained MPC) and the LMIs (50) to assure the stability of online implemented observer. In summary, the observer is designed and

$$\begin{bmatrix} \begin{pmatrix} A_j X_1 - BFX_1 + \\ X_1 A_j^T - X_1 F^T \mid B^T \end{pmatrix} & * & * & * \\ \begin{pmatrix} \left(A_i - A_j\right) X_1 \\ -X_2 C^T L_j^T \end{pmatrix} & \begin{pmatrix} A_i X_2 - L_j C X_2 + \\ X_2 A_i^T - X_2 C^T L_j^T \end{pmatrix} & * & * \\ 0 & B^T & -\gamma^2 I * & \\ CX_1 & CX_2 & 0 & -I \end{bmatrix} < 0. \quad (42)$$

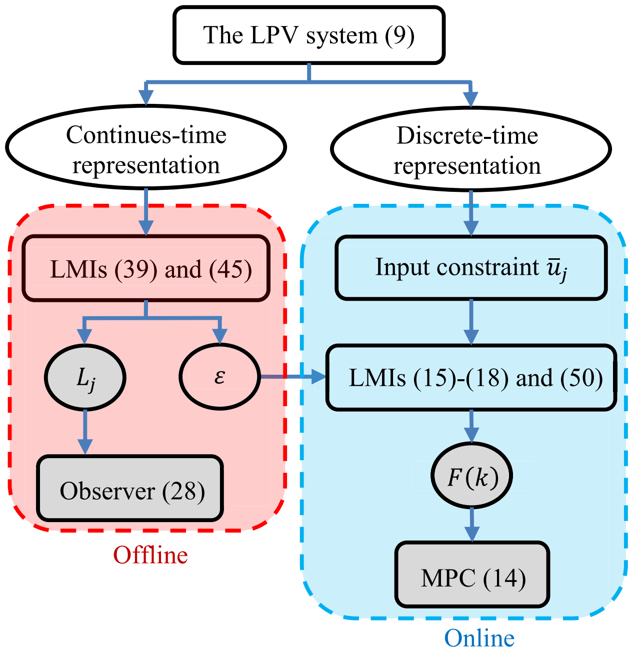


**FIGURE 4.** Total flowchart of the proposed method.

the parameter $\varepsilon$ is found offline. Then, this parameter as well as the control amplitude upper bounds are considered in the online procedure to design the MPC at each instance.

*Remark 1 (Advantages of the proposed approach):* By reviewing the state-of-the-art methods, it is inferred that few approaches consider the issue of inexactly measured scheduling parameters in observer-based MPC. These approaches have two drawbacks in general. I) The overall observer-based controller design conditions are not derived in terms of strict LMIs. Thereby, it is not possible to find the optimal solution and some parameters must be chosen by trial and error. II) The LMIs must be solved online to obtain both the observer and controller gains. Thereby, the number of LMI variables and the online computational burden increase. III) The MPC and observer are designed based on continuous- or discrete-time frameworks. If a continuous-time is utilized, practical online computation can be a critical issue for analogously updating the controller. On the other hand, if a discrete-time observer is utilized, the inter-sampling values of the states are not accurately estimated. The proposed controller deals with the above-mentioned issues. In order to have an accurate control and estimation for continuous-time nonlinear systems, the LPV-MPC is designed discrete-time with ZOH; while, the LPV-observer is continuous-time to precisely estimate the states. On the other hand, in order to reduce the online computational burden, it is necessary to design the gains and unknown parameters offline as much as possible. In this regard, the observer is designed offline and the gains of MPC are designed online, as is evident in Figure 3. Furthermore, to assure the closed-loop system stability, additional constraint in Section III, part c is proposed. Since the number of additional constraints (50) is few, the online computational burden of MPC LMIs slightly increases.

**TABLE 1.** Parameters of powertrain system [4] and [46].

| | | |
|---|---|---|
| $J_m$ | inertia of motor | $0.01\,Kg\,m^2$ |
| $J_g$ | Inertia of gearbox | $1.1828\,Kg\,m^2$ |
| $J_w$ | Inertia of wheels | $5.38\,Kg\,m^2$ |
| $c_m$ | Motor damping | $0.15\,Nm\,s/rad$ |
| $c_f$ | Driveshaft damping | $42\,Nm\,s/rad$ |
| $k_f$ | Driveshaft stiffness | $6000\,Nm\,s/rad$ |
| $c_a$ | Linear factor of air drag | $2.7\,Nm\,s/rad$ |
| $i_g$ | Gear ratio | 3.778 |
| $i_o$ | Final drive ratio | 3.667 |
| $m_v$ | Vehicle mass | $1094\,Kg$ |
| $r_w$ | Wheel radius | $0.281\,m$ |
| $\rho_{air}$ | Air density | $1.2\,Kg/m^3$ |
| $c_d$ | air drag coefficient | 0.3 |
| $A_f$ | Vehicle front area | $2.7\,m^2$ |
| $g$ | Gravitational acceleration | $9.81\,m/s^2$ |

## IV. SIMULATION RESULTS

In this section, the proposed Theorems 1 and 2 with (45) and (50) are applied to CAMT (1). The first-order Euler approximation constant is set as $T = 0.01(sec)$. Using Theorem 2, the following gains are achieved:

$$\begin{aligned} L_1 &= [135.2528 \quad 483.3522 \quad -0.0569]^T \\ L_2 &= [127.6370 \quad 461.3938 \quad -0.0469]^T \end{aligned} \tag{51}$$

The rotation speed of the gearbox output shaft (i.e. $x_2$) is measurable and the desired reference is the rotation speed of the wheel (i.e. $\omega_m^*$). Based on (1), the error $\tilde{x}_2(t)$ is obtained as $\tilde{x}_2(t) = x_2(t) - \omega_w^* = x_2(t) - \omega_m^*/i_g i_o$. The nominal values of the CAMT parameters are outlined in Table 1. Moreover, the aerodynamic parameters of the vehicle change at the instant $t = 1(sec)$. Since the time-varying parameter $\theta(t)$ is the function of these unmeasurable parameters, it can be considered as an inexact measurable variable. In the simulation, the following values are considered:

$$For\ t < 1: \begin{cases} \rho_{air} = 1.2 \\ C_d = 0.3 \\ A_f = 2.7 \end{cases} \quad For\ t \geq 1: \begin{cases} \rho_{air} = 1.4 \\ C_d = 0.4 \\ A_f = 2.6. \end{cases} \tag{52}$$

To show the performance improvement of the proposed approach over the other state-of-the-art approaches, the suggested method is compared with [4]. In [4], a discrete-time state feedback controller for the CAMT with time delay is considered and sufficient controller design constraints to assure robust stability and to improve passenger comfort are presented in terms of LMIs. To achieve a fair comparison, in the LMIs of [4], the time delay is set zero. Additionally, in that approach, it is assumed that the aerodynamic parameters are known. Thereby, for the nominal CAMT system, the

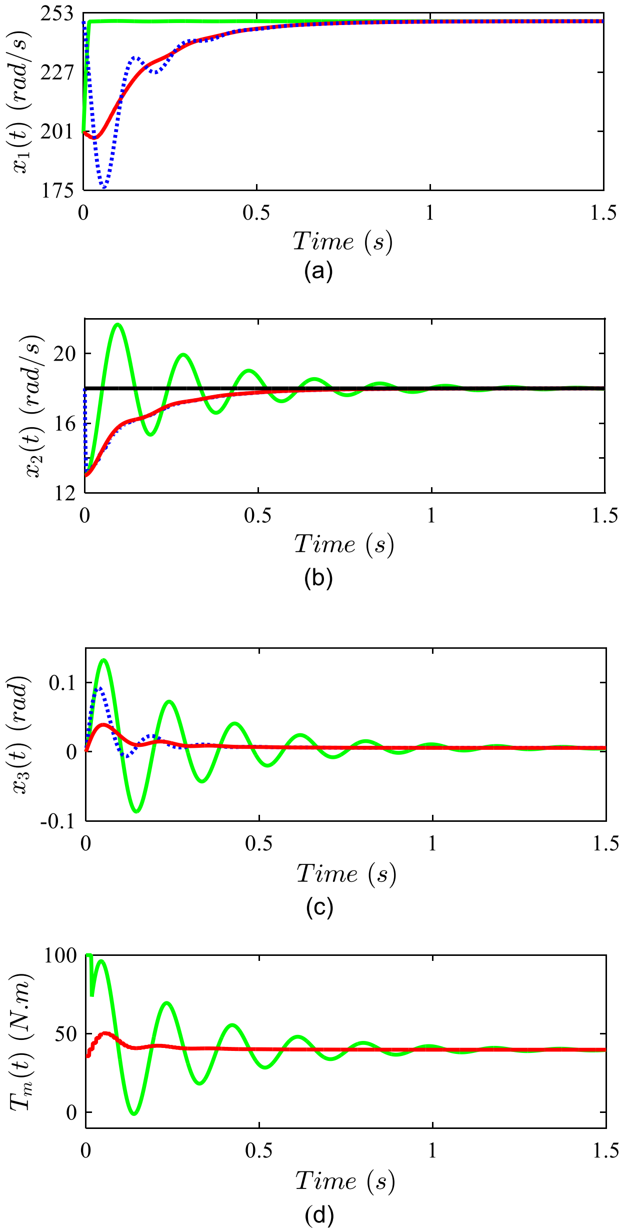


**FIGURE 5.** **The closed-loop CAMT system_ Scenario 1 (desired reference by solid black line, the actual state by solid red line, the estimation by the dotted blue line, and ref. [4] by solid green line). (a) The first state, (b) second state, (c) Third state, (d) Control input.**

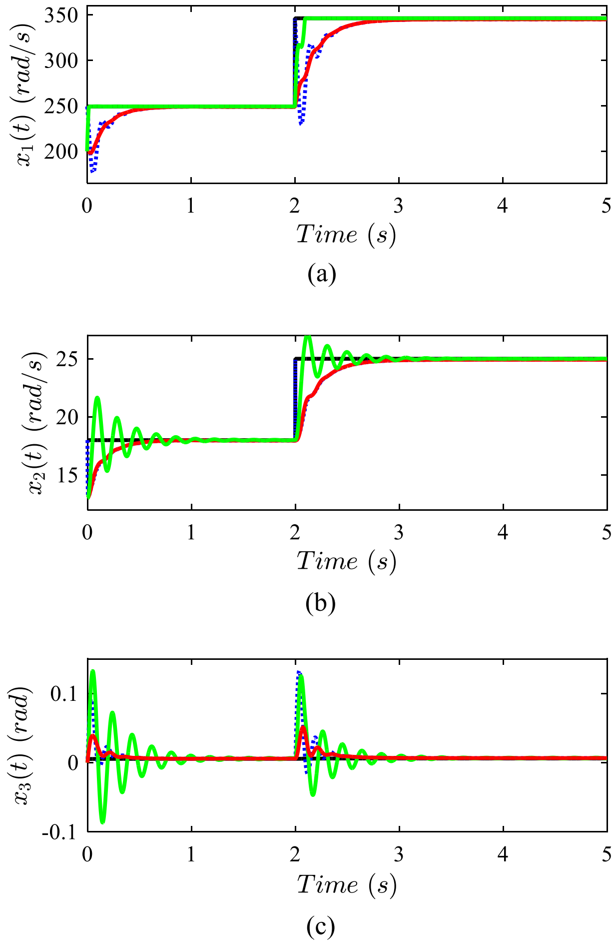


**FIGURE 6.** **The closed-loop CAMT system_ Scenario 2 (desired reference by solid black line, the actual state by solid red line, the estimation by the dotted blue line, and ref. [4] by solid green line). (a) The first state, (b) second state, (c) Third state.**

controller gain of [4] is computed as follows:

$$K = [-15.7996 \quad 11.2555 \quad 444.4310]. \tag{53}$$

In the following, two scenarios of constant and stepwise desired reference for the vehicle are considered.

### A. SCENARIO 1 (CRUISE CONTROL WITH CONSTANT SPEED)

The desired reference and initial conditions are $\omega_w^* = \frac{\omega_m^*}{i_g i_o} = 18(rad/s)$, $x(0) = \begin{bmatrix} 200 & 13 & 0 \end{bmatrix}^T$, and $\hat{x}(0) = \begin{bmatrix} 0 & 0 & 0 \end{bmatrix}^T$. Based on the constraint (8), and nominal values of Table 2, the lower and upper bounds are chosen as $\bar{\theta} = -\underline{\theta} = 0.58$. The closed-loop system responses, estimations of the observer, and the control input $T_m$ are given in Figure 5., which verifies that the proposed inexact observer-based controller successfully makes the closed-loop system states to track the desired values, even by using only one state variable for feedback and considering variations in the parameters $\rho_{air}$, $C_d$ and $A_f$.

As can be seen in Figure 5., although the speed of motor rotation tracking performance is improved by [4], the PEV experiences oscillation in all of its states. These oscillations degrade passenger comfort. Further, the control signal amplitude of [4] is two times larger than the proposed approach. Also, the proposed approach only uses the second system state as the measurement; meanwhile, the approach of [4] utilizes all states.

### B. SCENARIO 2 (STEPWISE DESIRED SPEED REFERENCE)

To show the performance of the developed controller and [4], it is assumed that the desired reference for the wheel rotation speed changes from $18(rad/s)$ to $25(rad/s)$ at $t = 2$ seconds. The observer gains and the aerodynamic parameters are the same as (51) and (52). Figure 6 shows the state evolution of

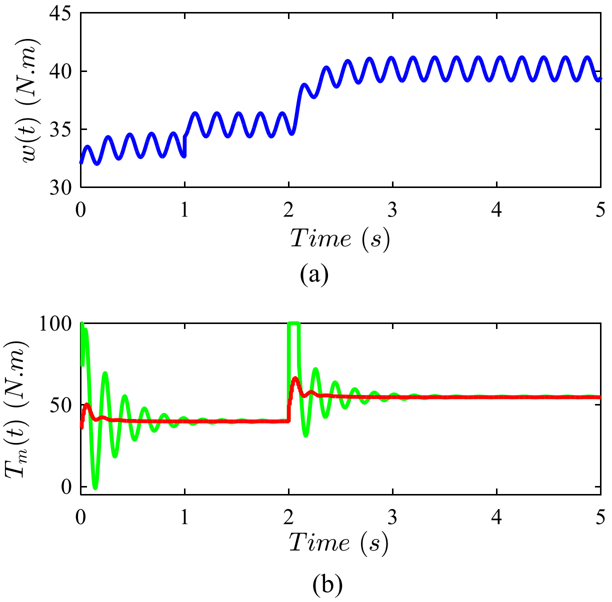


**FIGURE 7.** **The closed-loop CAMT system_ Scenario 2 (the proposed approach by solid red line and ref. [4] by solid green line). (a) The external disturbance, (b) Control input.**

the CAMT system. As can be seen in Figure 6, the proposed approach results in a smaller deviation of $x_3$ than that of [4], which increases passenger comfort when the vehicle speed changes.

Moreover, the control input and the external disturbance input are illustrated in Figure 7. As can be seen in Figure 7(a), the external disturbance is related to the aerodynamic parameters and vehicle speed. Further, the control input based on the approach [4] has a higher amplitude than the developed approach and reaches its upper bound amplitude.

## V. CONCLUSION

This paper proposed a novel observer-based MPC controller with inexactly measured scheduling parameters for nonlinear CAMT systems. The presented approach exploited the polytopic LPV model as an effective approach to assure the stability of the nonlinear observer and MPC lonely and the overall closed-loop system. Sufficient conditions of controller and observer were restated by LMIs. To make the developed approach accurate, the continuous-time (discrete-time) LPV-observer (LPV-MPC) was designed offline (online). To design the LPV-observer, the SVD of the output matrix was utilized to facilitate deriving convex constraints. Moreover, a constrained one-step-ahead LPV-MPC was developed. Whereas the separation principle was not held, additional constraints were exerted on both controller and observer LMIs to deal with the interactions between the observer and controller. Finally, numerical simulations were carried out and comparative results illustrated the merits of the developed approach in increasing the passenger comfort and PEV speed regulation for the considered CAMT case study. For future work, considering uncertainty in the observer-based controller design procedure is suggested. Extending the obtained results to a tube-based MPC and non-quadratic Lyapunov functions is recommended.

## REFERENCES

[1] A. Della Gatta, L. Iannelli, M. Pisaturo, A. Senatore, and F. Vasca, "A survey on modeling and engagement control for automotive dry clutch," *Mechatronics*, vol. 55, pp. 63–75, Nov. 2018, doi: 10.1016/j.mechatronics.2018.08.002.

[2] X. Wang, L. Li, K. He, and C. Liu, "Dual-loop self-learning fuzzy control for AMT gear engagement: Design and experiment," *IEEE Trans. Fuzzy Syst.*, vol. 26, no. 4, pp. 1813–1822, Aug. 2018, doi: 10.1109/TFUZZ.2017.2779102.

[3] S. Tamada, D. Bhattacharjee, and P. K. Dan, "Review on automatic transmission control in electric and non-electric automotive powertrain," *Int. J. Vehicle Perform.*, vol. 6, no. 1, p. 98, 2020, doi: 10.1504/IJVP.2020.104500.

[4] X. Zhu, H. Zhang, D. Cao, and Z. Fang, "Robust control of integrated motor-transmission powertrain system over controller area network for automotive applications," *Mech. Syst. Signal Process.*, vols. 58–59, pp. 15–28, Jun. 2015, doi: 10.1016/j.ymssp.2014.11.011.

[5] Y. Luo and D. Tan, "Lightweight design of an in-wheel motor using the hybrid optimization method," *Proc. Inst. Mech. Eng., D, J. Automobile Eng.*, vol. 227, no. 11, pp. 1590–1602, Nov. 2013, doi: 10.1177/0954407013497194.

[6] M. A. Miller, A. G. Holmes, B. M. Conlon, and P. J. Savagian, "The GM 'Voltec' 4ET50 multi-mode electric transaxle," *SAE Int. J. Engines*, vol. 4, no. 1, pp. 1102–1114, Apr. 2011, doi: 10.4271/2011-01-0887.

[7] M. Li, Z. Zhao, J. Fan, and J. Gao, "Estimation of transmission input&output shaft torque and drive wheel speed for compound power split powertrain based on unknown input observer," *IEEE Trans. Veh. Technol.*, vol. 69, no. 5, pp. 4883–4893, May 2020, doi: 10.1109/TVT.2020.2975085.

[8] W. Cao, Y. Wu, Y. Chang, Z. Liu, C. Lin, Q. Song, and A. Szumanowski, "Speed synchronization control for integrated automotive motor-transmission powertrains over CAN through a co-design methodology," *IEEE Access*, vol. 6, pp. 14106–14117, 2018, doi: 10.1109/ACCESS.2018.2810941.

[9] M. H. Khooban, N. Vafamand, T. Niknam, T. Dragicevic, and F. Blaabjerg, "Model-predictive control based on Takagi–Sugeno fuzzy model for electrical vehicles delayed model," *IET Electr. Power Appl.*, vol. 11, no. 5, pp. 918–934, 2017, doi: 10.1049/iet-epa.2016.0508.

[10] N. Vafamand, M. M. Arefi, M. H. Khooban, T. Dragicevic, and F. Blaabjerg, "Nonlinear model predictive speed control of electric vehicles represented by linear parameter varying models with bias terms," *IEEE J. Emerg. Sel. Topics Power Electron.*, vol. 7, no. 3, pp. 2081–2089, Sep. 2019, doi: 10.1109/JESTPE.2018.2884346.

[11] X. Zhu and W. Li, "Takagi–Sugeno fuzzy model based shaft torque estimation for integrated motor–transmission system," *ISA Trans.*, vol. 93, pp. 14–22, Oct. 2019, doi: 10.1016/j.isatra.2019.03.002.

[12] C.-Y. Tseng and C.-H. Yu, "Advanced shifting control of synchronizer mechanisms for clutchless automatic manual transmission in an electric vehicle," *Mechanism Mach. Theory*, vol. 84, pp. 37–56, Feb. 2015, doi: 10.1016/j.mechmachtheory.2014.10.007.

[13] X. Zhu, H. Zhang, J. Xi, J. Wang, and Z. Fang, "Robust speed synchronization control for clutchless automated manual transmission systems in electric vehicles," *Proc. Inst. Mech. Eng., D, J. Automobile Eng.*, vol. 229, no. 4, pp. 424–436, Mar. 2015, doi: 10.1177/0954407014546431.

[14] M. Ghaedi, F. Bayat, A. Fekih, and S. Mobayen, "Robust performance improvement of lateral motion in four-wheel independent-drive electric vehicles," *IEEE Access*, vol. 8, pp. 203146–203157, 2020, doi: 10.1109/ACCESS.2020.3037119.

[15] X. Zhu, H. Zhang, and Z. Fang, "Speed synchronization control for integrated automotive motor–transmission powertrain system with random delays," *Mech. Syst. Signal Process.*, vols. 64–65, pp. 46–57, Dec. 2015, doi: 10.1016/j.ymssp.2015.04.001.

[16] M. S. R. Mousavi, H. V. Alizadeh, and B. Boulet, "Estimation of synchromesh frictional torque and output torque in a clutchless automated manual transmission of a parallel hybrid electric vehicle," *IEEE Trans. Veh. Technol.*, vol. 66, no. 7, pp. 5531–5539, Jul. 2017, doi: 10.1109/TVT.2016.2619915.

[17] P. D. Walker, Y. Fang, and N. Zhang, "Dynamics and control of clutchless automated manual transmissions for electric vehicles," *J. Vib. Acoust.*, vol. 139, no. 6, Jul. 2017, Art. no. 061005, doi: 10.1115/1.4036928.

[18] J. Liang, H. Yang, J. Wu, N. Zhang, and P. D. Walker, "Power-on shifting in dual input clutchless power-shifting transmission for electric vehicles," *Mechanism Mach. Theory*, vol. 121, pp. 487–501, Mar. 2018, doi: 10.1016/j.mechmachtheory.2017.11.004.

[19] S. Iqbal, A. Xin, M. U. Jan, M. A. Abdelbaky, H. U. Rehman, S. Salman, S. A. A. Rizvi, and M. Aurangzeb, "Aggregation of EVs for primary frequency control of an industrial microgrid by implementing grid regulation & charger controller," *IEEE Access*, vol. 8, pp. 141977–141989, 2020, doi: 10.1109/ACCESS.2020.3013762.

[20] N. Vafamand and A. Khayatian, "Model predictive-based reset gain-scheduling dynamic control law for polytopic LPV systems," *ISA Trans.*, vol. 81, pp. 132–140, Oct. 2018, doi: 10.1016/j.isatra.2018.08.006.

[21] X. Ping, S. Yang, P. Wang, and Z. Li, "An observer-based output feedback robust MPC approach for constrained LPV systems with bounded disturbance and noise," *Int. J. Robust Nonlinear Control*, vol. 30, no. 4, pp. 1512–1533, Mar. 2020, doi: 10.1002/rnc.4836.

[22] Q. Tran Dinh, S. Gumussoy, W. Michiels, and M. Diehl, "Combining convex–concave decompositions and linearization approaches for solving BMIs, with application to static output feedback," *IEEE Trans. Autom. Control*, vol. 57, no. 6, pp. 1377–1390, Jun. 2012, doi: 10.1109/TAC.2011.2176154.

[23] X. Ping, S. Yang, B. Ding, T. Raïssi, and Z. Li, "Observer-based output feedback robust MPC via zonotopic set-membership state estimation for LPV systems with bounded disturbances and noises," *J. Franklin Inst.*, vol. 357, no. 11, pp. 7368–7398, Jul. 2020, doi: 10.1016/j.jfranklin.2020.05.014.

[24] X. Ping, "Output feedback robust MPC based on off-line observer for LPV systems via quadratic boundedness," *Asian J. Control*, vol. 19, no. 4, pp. 1641–1653, Jul. 2017, doi: 10.1002/asjc.1469.

[25] X. Ping and B. Ding, "Off-line approach to dynamic output feedback robust model predictive control," *Syst. Control Lett.*, vol. 62, no. 11, pp. 1038–1048, Nov. 2013, doi: 10.1016/j.sysconle.2013.07.011.

[26] Y. Song, Z. Wang, S. Liu, and G. Wei, "N-step MPC for systems with persistent bounded disturbances under SCP," *IEEE Trans. Syst., Man, Cybern. Syst.*, vol. 50, no. 11, pp. 4762–4772, Nov. 2020, doi: 10.1109/TSMC.2018.2862406.

[27] J. Wang and Y. Song, "Resilient RMPC for cyber-physical systems with polytopic uncertainties and state saturation under TOD scheduling: An ADT approach," *IEEE Trans. Ind. Informat.*, vol. 16, no. 7, pp. 4900–4908, Jul. 2020, doi: 10.1109/TII.2019.2938889.

[28] B. Ding and H. Pan, "Output feedback robust MPC for LPV system with polytopic model parametric uncertainty and bounded disturbance," *Int. J. Control*, vol. 89, no. 8, pp. 1554–1571, Aug. 2016, doi: 10.1080/00207179.2016.1138144.

[29] F. L. Estrada, J.-C. Ponsart, D. Theilliol, and C. M. Astorga-Zaragoza, "Robust $H_{-}/H_{\infty}$ fault detection observer design for descriptor-LPV systems with unmeasurable gain scheduling functions," *Int. J. Control*, vol. 88, no. 11, pp. 2380–2391, 2015.

[30] A. Sadeghzadeh, "Gain-scheduled filtering for linear parameter-varying systems using inexact scheduling parameters with bounded variation rates," *Int. J. Robust Nonlinear Control*, vol. 26, no. 13, pp. 2864–2879, Sep. 2016.

[31] P. Park, N. K. Kwon, and B. Y. Park, "State-feedback control for LPV systems with interval uncertain parameters," *J. Franklin Inst.*, vol. 352, no. 11, pp. 5214–5225, Nov. 2015, doi: 10.1016/j.jfranklin.2015.08.025.

[32] M. Sato, "Gain-scheduled flight controller using bounded inexact scheduling parameters," *IEEE Trans. Control Syst. Technol.*, vol. 26, no. 3, pp. 1074–1082, May 2018.

[33] I. E. Kose and F. Jabbari, "Control of LPV systems with partly measured parameters," *IEEE Trans. Autom. Control*, vol. 44, no. 3, pp. 658–663, Mar. 1999.

[34] M. Abbasghorbani and M. H. Asemani, "Induced $L_2$-norm observer-based controller design for continuous-time polytopic LPV systems," in *Proc. 5th Int. Conf. Control, Instrum., Autom. (ICCIA)*, Nov. 2017, pp. 103–107, doi: 10.1109/ICCIAutom.2017.8258661.

[35] C. M. Agulhari, E. S. Tognetti, R. C. L. F. Oliveira, and P. L. D. Peres, "$H_{\infty}$ dynamic output feedback for LPV systems subject to inexactly measured scheduling parameters," in *Proc. Amer. Control Conf.*, Washington, DC, USA, Jun. 2013, pp. 6060–6065, doi: 10.1109/ACC.2013.6580788.

[36] M. Sato, "One-shot design of performance scaling matrices and observer-based gain-scheduled controllers depending on inexact scheduling parameters," *Syst. Control Lett.*, vol. 137, Mar. 2020, Art. no. 104632, doi: 10.1016/j.sysconle.2020.104632.

[37] M. Abbasghorbani, M. H. Asemani, N. Vafamand, and S. Mobayen, "Inexact induced L2 observer-based control of polytopic LPV systems: Application to clutchless automated manual transmission of pure electric vehicles," *IET Control Technol. Appl.*, 2021.

[38] M. H. Asemani and V. J. Majd, "A robust $H_{\infty}$ observer-based controller design for uncertain T–S fuzzy systems with unknown premise variables via LMI," *Fuzzy Sets Syst.*, vol. 212, pp. 21–40, Feb. 2013, doi: 10.1016/j.fss.2012.07.008.

[39] G. Lucente, M. Montanari, and C. Rossi, "Modelling of an automated manual transmission system," *Mechatronics*, vol. 17, nos. 2–3, pp. 73–91, Mar. 2007, doi: 10.1016/j.mechatronics.2006.11.002.

[40] J. Hu and B. Ding, "One-step ahead robust MPC for LPV model with bounded disturbance," *Eur. J. Control*, vol. 52, pp. 59–66, Mar. 2020, doi: 10.1016/j.ejcon.2019.09.004.

[41] J.-H. Park, T.-H. Kim, and T. Sugie, "Output feedback model predictive control for LPV systems based on quasi-min–max algorithm," *Automatica*, vol. 47, no. 9, pp. 2052–2058, Sep. 2011, doi: 10.1016/j.automatica.2011.06.015.

[42] B. Kaviarasan, O. M. Kwon, M. J. Park, and R. Sakthivel, "Composite synchronization control for delayed coupling complex dynamical networks via a disturbance observer-based method," *Nonlinear Dyn.*, vol. 99, no. 2, pp. 1601–1619, Jan. 2020, doi: 10.1007/s11071-019-05379-7.

[43] D. Aravindh, R. Sakthivel, B. Kaviarasan, S. M. Anthoni, and F. Alzahrani, "Design of observer-based non-fragile load frequency control for power systems with electric vehicles," *ISA Trans.*, vol. 91, pp. 21–31, Aug. 2019, doi: 10.1016/j.isatra.2019.01.031.

[44] F. Wu, X. H. Yang, A. Packard, and G. Becker, "Induced $L_2$-norm control for LPV systems with bounded parameter variation rates," *Int. J. Robust Nonlinear Control*, vol. 6, nos. 9–10, pp. 983–998, Nov. 1996.

[45] D. W. C. Ho and G. Lu, "Robust stabilization for a class of discrete-time non-linear systems via output feedback: The unified LMI approach," *Int. J. Control*, vol. 76, no. 2, pp. 105–115, Jan. 2003.

[46] C. F. Caruntu, M. Lazar, R. H. Gielen, P. P. J. van den Bosch, and S. Di Cairano, "Lyapunov based predictive control of vehicle drivetrains over CAN," *Control Eng. Pract.*, vol. 21, no. 12, pp. 1884–1898, Dec. 2013, doi: 10.1016/j.conengprac.2012.05.012.


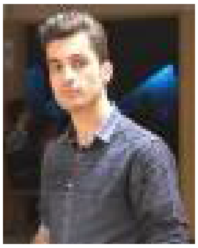

**MOHAMMAD SAEID AKBARI** was born in Ilam, Iran, in 1993. He received the bachelor's degree in electrical engineering from Hamedan Technical University, in 2017. He is currently pursuing the M.Sc. degree in control engineering with Shiraz University. His research interests include LPV control, robust control, and model predictive control.

**MOHAMMAD HASSAN ASEMANI** (Member, IEEE) received the B.Sc. degree from the Electrical Engineering Department, Shiraz University, Shiraz, Iran, in 2006, and the M.Sc. and Ph.D. degrees in control engineering from the Electrical and Computer Engineering Department, Tarbiat Modares University, Tehran, Iran, in 2008 and 2012, respectively. Since 2017, he has been an Associate Professor with the Power and Control Department, Shiraz University. His research interests include T-S fuzzy control, linear parameter-varying (LPV) systems, fractional-order systems, observer-based control, and linear matrix inequalities in control. He received the One-Year Scholarship Award of the Ministry of Science, Research and Technology of Iran in 2012.

**NAVID VAFAMAND** received the B.Sc. degree in electrical engineering and the M.Sc. degree in control engineering from the Shiraz University of Technology, Shiraz, Iran, in 2012 and 2014, respectively, and the Ph.D. degree in control engineering from Shiraz University, Shiraz, in 2019. He was a Ph.D. Visiting Student with the Department of Energy Technology, Aalborg University, Denmark, from 2017 to 2018. He currently holds a Postdoctoral Researcher position with Shiraz University. He has coauthored more than 90 international conference and journal articles and two book chapters. He is also an active reviewer in several journals. His research interests include Takagi–Sugeno (TS) fuzzy models, predictive control, and dc–dc microgrids.

**SALEH MOBAYEN** (Member, IEEE) received the B.Sc. and M.Sc. degrees in control engineering from the University of Tabriz, Tabriz, Iran, in 2007 and 2009, respectively, and the Ph.D. degree in control engineering from Tarbiat Modares University, Tehran, Iran, in January 2013. From February 2013 to December 2018, he was as an Assistant Professor and a Faculty Member with the Department of Electrical Engineering, University of Zanjan, Zanjan, Iran. Since December 2018, he has been an Associate Professor of control engineering with the Department of Electrical Engineering, University of Zanjan. He currently collaborates with the National Yunlin University of Science and Technology as an Associate Professor of the Future Technology Research Center. He has published several articles in the national and international journals. He is also a member of the IEEE Control Systems Society and also serves as a member of program committee for several international conferences. He is also the Associate Editor of *Artificial Intelligence Review*, *International Journal of Control, Automation and Systems*, *Circuits, Systems, and Signal Processing*, *Simulation*, *Measurement and Control*, *International Journal of Dynamics and Control*, and *SN Applied Sciences*; an Academic Editor of *Complexity* and *Mathematical Problems in Engineering*; and other international journals. His research interests include control theory, sliding mode control, robust tracking, non-holonomic robots, and chaotic systems.

**AFEF FEKIH** (Senior Member, IEEE) received the B.S., M.S., and Ph.D. degrees in electrical engineering from the National Engineering School of Tunis, Tunisia, in 1995, 1998, and 2002, respectively. She is currently a Full Professor with the Department of Electrical and Computer Engineering and the Chevron/BORSF Professor of engineering with the University of Louisiana at Lafayette. Her research interests include control theory and applications, including nonlinear and robust control, optimal control, fault tolerant control with applications to power systems, wind turbines, unmanned vehicles, and automotive engines. She is also a member of the IEEE Control Systems Society and the IEEE Women in Control Society.